Source mechanisms of mining-induced seismicity at Kloof Gold Mine, South Africa – moment tensor analysis of $M_L \geq 1.5$ events

Richard Masethe
Rock Engineering and Seismology Department, Sibanye-Stillwater Limited, Johannesburg, South Africa

Raymond Durrheim
School of Geosciences, University of the Witwatersrand, Johannesburg, South Africa

Musa Manzi
School of Geosciences, University of the Witwatersrand, Johannesburg, South Africa

ABSTRACT: Mining-induced seismic events in South African deep-level gold mines cause hazardous working conditions, damage infrastructure, delay production and pose a risk to miners. A good understanding of seismic source mechanisms is needed for seismic data to be used efficiently and effectively for mine planning purposes. A comprehensive study of mining-induced seismic events (M_L1.5 – 3.3) that caused damage to stopes at Kloof Gold Mine is described. The source mechanisms of 88 events were calculated. All events were located within the central part of the in-mine seismic network, enabling reliable moment tensors to be determined. It was found that approximately equal numbers of events were related to mining-related structures (such as pillars and abutments) and to geological structures (such as faults and dykes).

Keywords: seismicity, mining-induced, moment tensors, Kloof Gold Mine.

1 INTRODUCTION

As mines get deeper and the stoped-out volumes expand in size, rock stresses and consequent mining-induced seismic activity will generally increase and rockbursts may become a major hazard. The extensive tabular stopes typical of deep South African gold mines are vulnerable to shaking and damage. An understanding of the source mechanisms of mining-induced seismic events is vital if we are to mitigate the risk of rockbursts. The objective of this study is to improve our understanding of the source mechanisms of the large seismic events that occur when mining the Ventersdorp Contact Reef (VCR) in Kloof Gold Mine to assist in the development and implementation of appropriate mining and support strategies.

Kloof Gold Mine is located in the West Rand goldfield of the Witwatersrand Basin, 65 km southwest of the city of Johannesburg (Figure 1). Four shafts produce ore from pillars and open ground. The Ventersdorp Contact Reef (VCR) is the primary economic gold-bearing horizon, while the relatively low-grade Kloof, Libanon and Middelvlei reefs are exploited on a small scale. The VCR orebody dips toward the southeast at approximately 21° and is cut by numerous faults and dykes. Mining occurs at depths ranging from 1300 m to 3900 m below the surface, with an average channel width of 1.34 m and a mining height of 1.8 m. The sequential grid mining layout is used in

the study area with 30-m-wide dip pillars spaced at 120 m. Kloof Gold Mine has a local underground seismic network that continuously monitors critical areas. It comprises 40 4.5 Hz tri-axial sensors that sample at a rate of 6 kHz. The detection threshold is approximately M_L-3.0. All the sensors are installed in boreholes drilled from mine tunnels, resulting in a roughly planar sensor configuration (Figure 2(a & b)). The typical location error for magnitude M_L1.0 is 30 m on plan and larger on depth (Figure 2(d)).

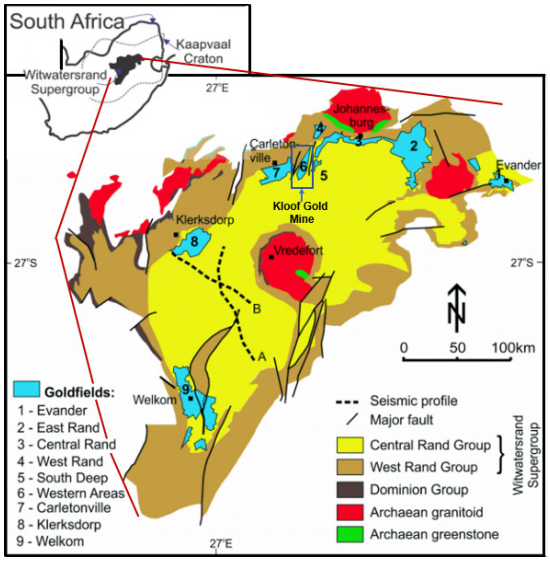

Figure 1. Location of Kloof Gold Mine, West Rand Goldfield, Witwatersrand Basin (after Frimmel 2019).

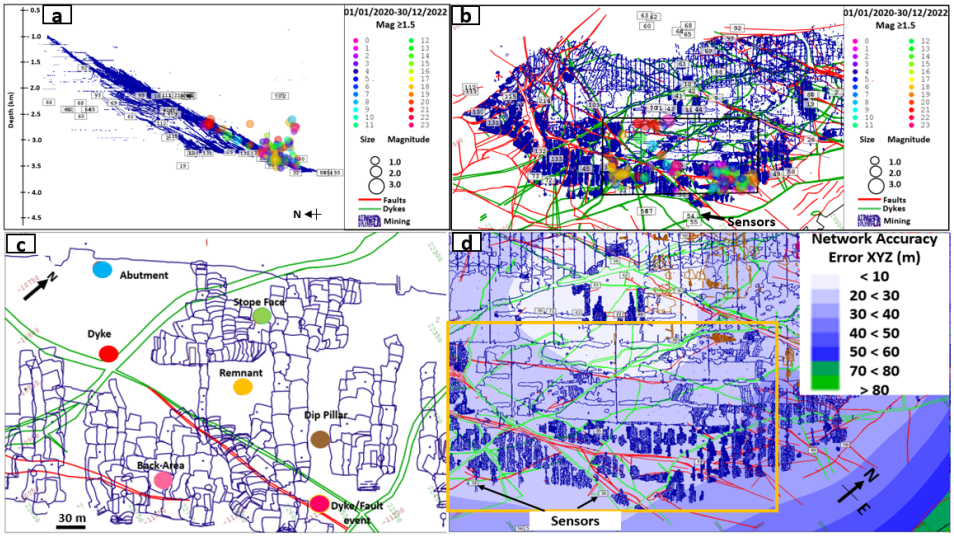

Figure 2. (a) Cross section plot showing stopes, sensors and seismic events, (b) spatial distribution of M≥1.5 seismic events (c) Main seismic emission sources at Kloof Gold Mine, and (d) Location accuracy. An orange rectangle encloses the study area.

2 ANALYSIS OF SEISMIC SOURCE MECHANISMS

All mining-related rock fracturing processes are accompanied by seismic energy emissions, although the energy may be too small to be detected by the monitoring system. In the underground mining environment, the most important processes are the formation of shear fractures, slip along geological discontinuities, and the violent failure of a volume of rock (Jager & Ryder 1999). The main sources of seismic emissions at Kloof Gold Mine are shown in Figure 2(c). The mines' local magnitude scale

(M_L) is based on measurements of Energy and Moment calculated by the IMS seismic system derived from the Fourier spectra of seismograms. Medium to large magnitude events ($M_L \geq 1.5$) generally occur close to geological structures such as dykes and faults; or are associated with features of mining layouts such as abutments, stability pillars, remnants, and back areas (Figure 2(c)). Furthermore, poor mining geometry (such as face shapes with leads and lags that deviate from standards) can trigger seismic events close to working areas in stopes.

Moment tensor analysis is able provide valuable insight into the physical mechanisms of mining-induced seismic events (Gibowicz & Kijko 1994). Interpretation of the moment tensor gives insight into whether the rock mass failed in tension, compression, or shear, and indicates the direction of movement and the failure plane. It provides an improved determination of the orientation of the geological structures responsible for the seismic events. The moment tensor inversion software used by the Institute of Mine Seismology (IMS) system installed at Kloof Gold Mine is based on an algorithm published by Vavryčuk & Kuhn (2012). The algorithm makes use of the amplitude and polarity of the manually processed waveforms; thus reliable moment tensor results are dependent on installation procedures that ensure good coupling and accurate orientation of sensors, accurate picks of the first arrivals, high signal-to-noise ratio, accurate velocity model and good network coverage, amongst others. The Kloof seismic system is adequate (average system health is 96%, and borehole sensors are oriented within 0-5° of true north during installation) and use the mesh-layered velocity model, which was launched a few years ago. Because the noise level for a 4.5 Hz geophone sensor is $1x10^{-6}$ $m.s^{-1}$, the signal-to-noise ratio is 10 (as used in short-term average -STA and long-term average - LTA). Because mining hasn't changed substantially, a sensor orientation audit was performed as a one-time exercise that can be evaluated as needed. To reduce errors due to uncertainties in the velocity model and hypocenter location, only seismic events surrounded by sensors (a denser network) were chosen for this study (Figure 2b).

3 MOMENT TENSOR INVERSION

A dataset of 88 mining-related seismic events ($1.5 \leq M_L \leq 3.3$) was selected (Figure 2 (b)). To ensure the reliable calculation of moment tensors, the following procedure was followed. (i) Only events located within the central part of the in-mine seismic network and well-recorded at 20 or more sites were selected. (ii) Only waveforms with high signal to noise ratio and recorded by sensors verified to have a misfit angle of less than 20° (i.e. the angle between vector from the sensor to the seismic event and the polarized vector of the Primary wave arrival) were used. The misfit in the inversion might be due to poor site orientation, noisy polarity estimation, or ray bending near the fractured excavations due to inhomogeneity within the rock mass. All sites were verified whether the wave orientation aligns with the event-sensor direction. (iii) The first arrival times were carefully picked. (iv) An improved velocity model was used to locate the events. This is a single velocity model determined using a calibration blast. The model is usually updated when large events are fund to be mislocated. This is typically done every 3–5 years. The P-S picks were refined with subsequent checks and refinements until the location residual was reduced to less than 50 m or less than 3% of the average hypocentral distance (AHD).

Figure 4(a) shows the results of a typical moment tensor inversion: a low isotropic (ISO) component (19.7%) indicates a small volumetric deformation (burst) towards the source of the seismic event. The small compensated linear vector dipole (CLVD) component (1.7%) indicates that stope closure (uniaxial deformation) formed only a small part of the seismic event mechanism. The significant double couple (DC) component (78.6%) indicates that shear (slip), either on a fault or on a new fracture through intact rock, was a major contributor to the seismic event mechanism. The moment tensor's Fault Plane Solutions (FPS1, FPS2) suggest that the event was due to slip on a structure with a roughly EW strike (102° and 101°, respectively) but with contrasting dips (18°, 73°) and rakes (72°, -96°). An EW-striking fault has been mapped some 25 m from the seismic event location, which corresponds to the orientation of the Fault Plane Solution 1 striking 102° and dipping 18° (Figure 4 (b)). It should be noted that the accuracy of seismic event location is up to 30 m (for $M \geq 1.0$), so it is considered likely that the seismic event is related to a slip on this fault.

Moment tensor inversion results of events ranging in size from $1.5 \leq M_L \leq 3.3$ were superimposed on the mine map (Figure 4 (b)), along with mapped geological structures in the area of interest. Due to the fact that relatively small stress changes can trigger a seismic event, it is possible that seismic activity can be triggered at fairly large distances from mining (McKinnon 2006). The orientation of the seismically-capable structures (dykes, faults, abutments, dip pillars, etc.) were compared with the possible nodal planes of the focal mechanisms for each of the seismic events in Figure 4(b), providing insight into possible modes of failure. Solutions were rotated into the plane of the reef (ore body) which strikes NNE and dips ESE between 25° - 45°.

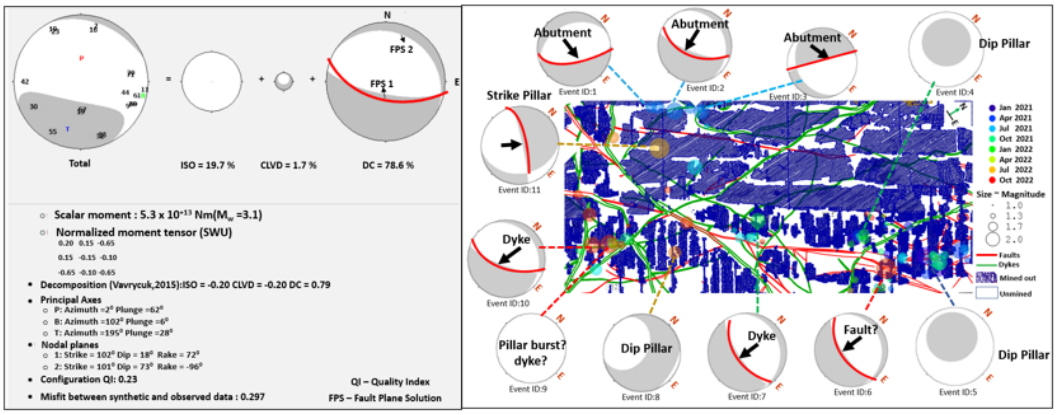

Figure 4 (a): Result of Moment Tensor Inversion. Principal Axes are Pressure (P), orthogonal to the slip vector (B) and Tension (T). SWU indicate "South-West Up". (b) Deviatoric focal mechanisms of selected $M_L \geq 1.5$ seismic events associated with various mining and geological elements at Kloof Gold Mine. The Moment Tensor is rotated into the plane of the reef; the red line indicates the Fault Plane Solution that aligns best with the mining elements.

The parameter describing the accepted fault plane solutions are listed in Table 1, in which nodal plane 1 is the fault plane and nodal plane 2 is the auxiliary plane. The parameters indicate the Moment tensor solutions, Fault Plane Solution, Decomposition components, Quality index, Misfit error and lastly the type of dominant faulting.

Table 1. Parameters of some calculated focal mechanism solutions (moment tensor and nodal planes).

Event ID	Moment Tensor Solutions			Fault Plane Solution 1 (FPS 1)	Fault Plane Solution 2 (FPS 2)	Decomposition Components		Quality Index	Misfit Error	Type of Dominant faulting
	Seismic event	Moment Tensor Components	Moment (Nm)	Strike/Dip/ Rake (°)	Strike/Dip/ Rake (°)	ISO (%)	DC (%)			
1	M_L= 2.5	M_{11}	-5.0 X 10^{11}	200/33/-106	39/58/-80	19.2	80.8	0.51	0.22	Normal Slip
		M_{22}	-2.8X 10^{12}							
		M_{33}	9,1 X 10^{12}							
		M_{12}	-1.5 X 10^{12}							
		M_{13}	2.8 X 10^{12}							
		M_{23}	1.8 X 10^{12}							
2	M_L=2.7	M_{11}	9 X 10^{11}	327/43/-41	89/63/-125	25.7	74.3	0.55	0.23	Normal Slip
		M_{22}	- 2.5 X 10^{12}							
		M_{33}	- 6.2 X 10^{12}							
		M_{12}	4.0 X 10^{11}							
		M_{13}	- 5.0 X 10^{12}							
		M_{23}	3.2 X 10^{12}							
3	M_L= 2.6	M_{11}	7.0 X 10^{11}	165/24/-107	3/67/-83	1.6	65.2	0.61	0.28	Normal Strike Slip
		M_{22}	4.9 X 10^{12}							
		M_{33}	- 4.9 X 10^{12}							
		M_{12}	2.2 X 10^{11}							
		M_{13}	2.6X 10^{12}							
		M_{23}	-4.9 X 10^{12}							

To investigate the source mechanism of the ensemble of events, the data were plotted on a Hudson source-type diagram (Figure 4 (a)). The Hudson diagram is a graphical representation of the seismic source based on two plotted parameters, T and K, which represent the relative proportion of constant volume deformation of the source (i.e., shear) and volume change (i.e., dilation/contraction) of the source, respectively (Hudson et al. 1989).

The deviation component of shear-type seismic occurrences was calculated to be more than 60%. Out of the 26 shear-type events, ~60% (15 of 26) indicated the dominant DC component (DC≥60%) with low CLVD. Most of these seismic events were plotted at a shallower depth than those with a dominant CLVD, which mostly occurred between 2800 - 3200 m, with a mean depth of 2900 m close to the reef horizon. Figure 4 (b) shows that pillars followed by abutment were the most frequent source of events of 1.5<ML<2. Events of ML > 2 occurred most frequently in the dykes and faulting.

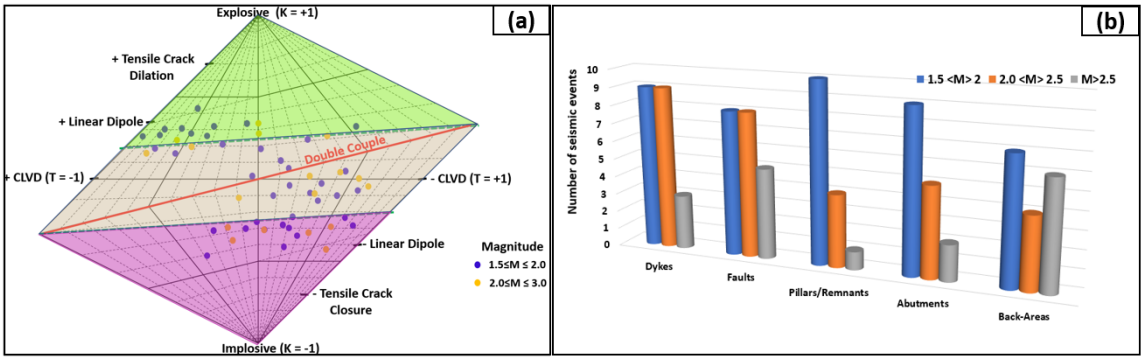

Figure 4: (a) Hudson diagrams plot with all source mechanisms. The Hudson diagram is divided into 3 regions: Upper region (Explosive), Central region (High DC) and Lower region (implosive). Black lines are contours of constant T (measure of deviatoric moment release, running from right to left) and K (measure of the change in volume, running from top to bottom). (b) Classes of seismic events according to their proximity to different source type.

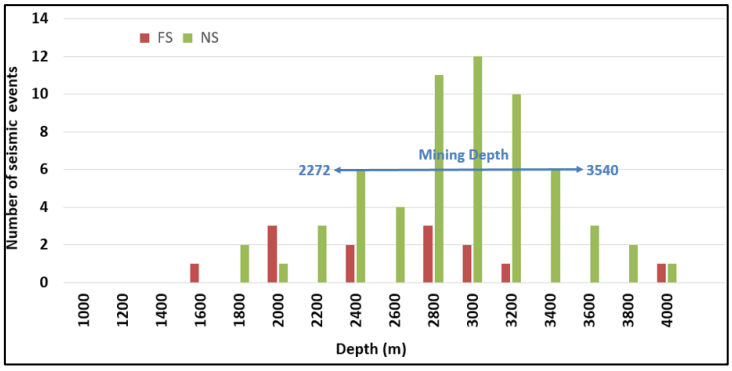

Figure 5. The distribution of seismic events source mechanisms in different mining levels within the VCR orebody. Brown and green represents the Fault Slip (FS) and Green Non-Shear (NS) sources, respectively.

4 DISCUSSION

The current analysis concentrates on a set of 88 events with $M_L \geq 1.5$ that occurred between 1 January 2021 and 31 December 2022, all located in the central part of the seismic network (Figure 2). Manual processing led to a combined set of source mechanism solutions of variable quality. The quality of each moment tensor solution has been quantified using the misfit between observed and synthetic waveforms and the 2D coverage of sensors.

The Moment Tensor Inversion solution of the selected and analysed seismic events (Figure 4(b)) highlighted that 60% -of the analyzed seismic events had a dominant shear component. Four events

(ID 1-4) plotted near a geological structure. However, the Fault Plane Solution did not align with the strike of the geological structure, but rather with the abutment of the irregularly-shaped pillars in the back areas. Due to mining activities, dynamic loading on the structure and the build-up of stress over time might have triggered these seismic events.

The Moment Tensor of three events (ID 5, 6, 9) was CLVD dominated, indicating that uniaxial deformation formed a significant part of the mechanism. This mechanism was typically associated with dynamic pillar failure and stope closure. This was consistent with the observation of dynamic closure on the support elements. The seismic events that are dominated by the volumetric component, could indicate a pillar burst. Their source mechanisms are characterized by a high degree of volumetric closure and a minor degree of pure shear. Typically, damage is limited to a single mining panel.

Three events (ID 7, 8, 11) were aligned with nearby geological structures. Their Moment Tensor solution supports the hypothesis that fault- and dyke-controlled seismic events have strong double-couple focal mechanisms. Their solutions implies an insignificant implosive isotropic component, with nodal planes aligned to the NE and ENE striking dykes and faults. The seismic event occurs within 10-30 m of these dykes and faults.

Overall, about half of the Moment Tensor solutions (52%) had a dominant (≥60%) DC component. Of these, 28% exhibit positive ISO and CLVD indicating tensile crack dilation ('explosions'), while 72% showed negative ISO and CLVD indicating tensile crack closure ('implosions'). The interpretations of the explosive or implosive point source model (isotropic component) links to the volume change process within the affected rock mass. Most of the observed seismic events within the area of interest are associated with reverse strike slip and normal slip.

5 CONCLUSIONS

The source mechanisms of 88 seismic events were calculated. All seismic events were located within the central part of the seismic network, enabling reliable moment tensors to be determined. It was found that approximately equal numbers of events were related to mining-related structures (such as pillars, back areas, and abutments) and to geological structures (such as faults and dykes).

REFERENCES

Frimmel, H. 2019. The Witwatersrand Basin and its gold deposits. In: *The Archaean geology of the Kaapvaal craton, southern Africa*, Kröner, A. & Hofmann, A. (eds), Regional Geology Reviews, pp. 255-275, Springer: Cham.

Gibowicz, S.J. & Kijko, A. 1994. An introduction to mining seismology. San Diego, California: Academic Press, Inc.

Hudson, J.A., Pearce, R.G. & Rogers, R.M. 1989. Source type plot for inversion of the moment tensor. *Journal of Geophysical Research: Solid Earth,* 94(B1), pp.765-774. https://doi.org/10.1029/JB094iB01p00765

Jager, A.J. & Ryder, J.A. 1999. A handbook on rock engineering practice for tabular hard rock mines. Safety in Mines Research Advisory Committee: Johannesburg.

McKinnon, S.D. 2006. Triggering of seismicity remote from active mining excavations. *Rock mechanics and rock engineering,* 39(3), pp. 255-279. DOI:10.1007/s00603-005-0072-5.

Masethe, R.T., Durrheim, R.J. & Manzi, M.S.D. 2022. Moment tensor analysis of four $M_L \geq 2.0$ seismic events that occurred at Kloof Gold Mine (South Africa) on 13 June 2017 and a statistical study of their fore- and aftershocks. In: *Proceedings of the 10th International Symposium on Rockburst & Seismicity in Mines*, Tucson, USA, 26-28 April 2022, Paper No. RASIM22-0413.

Masethe, R.T., Durrheim, R.J. & Manzi, M.S.D. 2022. Investigation of the source mechanisms of mining induced seismic events at Kloof Gold Mine, South Africa, In: *Proceedings of the 10th International Symposium on Rockburst & Seismicity in Mines*, Tucson, USA, 26-28 April 2022, Paper No. RASIM22-0511.

Vavryčuk, V. & Kühn, D. 2012. Moment tensor inversion of waveforms: a two-step time-frequency approach. *Geophysical Journal International,* 190(3), pp.1761-1776.